

Effect of Dehydration on Sulfate Coordination and Speciation at the Fe–(Hydr)oxide–Water Interface: A Molecular Orbital/Density Functional Theory and Fourier Transform Infrared Spectroscopic Investigation

Kristian W. Paul,* Michael J. Borda, James D. Kubicki,[†] and Donald L. Sparks

Department of Plant and Soil Sciences, 152 Townsend Hall, University of Delaware, Newark, Delaware 19716, and Department of Geosciences and Earth & Environmental Systems Institute, The Pennsylvania State University, University Park, Pennsylvania 16802

Received March 9, 2005. In Final Form: September 7, 2005

The effect of dehydration on the coordination and speciation of sulfate at the Fe–(hydr)oxide–H₂O interface was investigated using molecular orbital/density functional theory (MO/DFT) and Fourier transform infrared (FTIR) spectroscopy. IR frequency calculations were performed at the UB3LYP/6-31+G(d) level of theory for potential sulfate (bidentate bridging, monodentate, and H-bonded) and bisulfate (bidentate bridging and monodentate) surface complexes. MO/DFT calculated IR frequencies were compared to available IR literature results and attenuated total reflectance (ATR) FTIR spectra collected in our laboratory of sulfate adsorbed at the hematite–H₂O interface. IR frequency calculations performed using the larger 6-311+G(d,p) basis set resulted in minor frequency shifts that did not dramatically alter the agreement with experiment. This investigation proposes that sulfate undergoes a speciation change as a function of surface dehydration. A generalized model for the speciation change is proposed as follows. (1) At the Fe–(hydr)oxide–H₂O interface, sulfate adsorbs as a bidentate bridging or monodentate surface complex under most experimental conditions. (2) Upon surface dehydration, sulfate changes speciation to form bidentate bridging and/or monodentate bisulfate. However, surface dehydration does not yield 100% speciation change but leads to a mixture of sulfate and bisulfate. (3) The speciation change is reversible as a function of rehydration. The reversibility of the sulfate–bisulfate speciation change is chiefly determined by the local hydration environment of the O–H bond in bisulfate. Under dehydrated conditions, the O–H bond length is approximately 0.98 Å. The bond length substantially increases (bond strength decreases) to approximately 1.03 Å when the initial H-bond network is re-established through hydration, likely leading to deprotonation upon full mineral surface hydration.

1. Introduction

Certain hydrated mineral surfaces accumulate acidity (i.e., proton accumulation) as a function of drying, a process explained as resulting from dissociative water adsorption at polarizable metal cation sites.¹ Mineral surface acidification caused by drying modifies the redox properties and reactivity of Mn oxides^{2,3} and changes mineral surface charge density and metal cation adsorption capacity.⁴ The effect of dehydration (and subsequent proton accumulation) on the coordination and speciation of environmentally important oxyanions (e.g., sulfate, phosphate, arsenate, oxalate, etc.) at mineral surfaces has been relatively unexplored. An understanding of this natural process is critical to predicting oxyanion bioavailability and transport in geochemical and soil systems.

For nearly four decades, it has been understood that sulfate retention in acid soils occurs through a ligand-exchange mechanism involving hydroxyl and/or aquo surface functional groups associated predominantly with Fe– and Al–(hydr)oxides.^{5–8} Macroscopic adsorption

isotherm data from Aylmore et al.⁹ showed sulfate adsorption to Fe– and Al–(hydr)oxide surfaces was nearly irreversible, indicated by hysteresis between adsorption and desorption profiles.

In the 1970s, molecular-scale measurements of sulfate adsorption on a variety of Fe–(hydr)oxide surfaces were performed using transmission infrared (IR) spectroscopy.^{10,11} Through a combination of high affinity adsorption isotherms, surface-site availability estimates, and IR spectroscopic measurements, Parfitt and Smart¹¹ determined that sulfate formed a bidentate bridging surface complex. The assignment of the surface complex geometry was based upon the interpretation of IR spectra through symmetry arguments within the framework of group theory. Briefly, these specific symmetry arguments rely on the IR activity of the ν_1 fundamental and degree of degeneracy of the ν_3 fundamental as related to the S–O normal modes of sulfate. The IR activity of ν_1 and ν_3 depend on the point group of sulfate which determines its coordination environment (i.e., descent in symmetry of the T_d point group through its hierarchy of subgroups— C_{3v} , C_{2v} , etc.) In other words, the assignment of a surface

* To whom correspondence should be addressed. E-mail: kpaul@udel.edu.

[†] The Pennsylvania State University.

(1) Mortland, M. M.; Raman, K. V. *Clays Clay Miner.* **1968**, *16*, 393.
(2) Bartlett, R.; James, B. *Soil Sci. Soc. Am. J.* **1980**, *44*, 721.
(3) Ross, D. S.; Hales, H. C.; Shea-McCarthy, G. C.; Lanzirotti, A. *Soil Sci. Soc. Am. J.* **2001**, *65*, 736.
(4) Kennedy, C.; Smith, D. S.; Warren, L. A. *Geochim. Cosmochim. Acta* **2004**, *68*, 443.
(5) Chang, M. L.; Thomas, G. W. *Soil Sci. Soc. Am. J. Proc.* **1963**, *27*, 281.

(6) Chao, T. T.; Harward, M. E.; Fang, S. C. *Soil Science* **1962**, *94*, 276.

(7) Chao, T. T.; Harward, M. E.; Fang, S. C. *Soil Science* **1965**, *99*, 104.

(8) Jurinak, J. J. *Soil Science Soc. Am. Proc.* **1966**, *30*, 559.

(9) Aylmore, L. A. G.; Karim, M.; Quirk, J. P. *Soil Science* **1967**, *103*, 10.

(10) Parfitt, R. L.; Smart, R. S. C. *J. Chem. Soc., Faraday Trans. I* **1977**, *73*, 796.

(11) Parfitt, R. L.; Smart, R. S. C. *Soil Sci. Soc. Am. J.* **1978**, *42*, 48.

complex geometry was proposed on the basis of the number of observed S–O IR-active normal modes. Readers interested in details concerning group theory and its relationship with molecular geometry and complexation are referred to Nakamoto¹² and Carter.¹³

Turner and Kramer¹⁴ determined that sulfate adsorption to goethite (α -FeOOH) and hematite (α -Fe₂O₃) resulted partially in outer-sphere complexation (electrostatic attraction) but found a predominance of inner-sphere bidentate bridging sulfate combined with a possible, minor fraction of a monodentate structure. Infrared spectra of Turner and Kramer¹⁴ agreed reasonably well with those of Harrison and Berkheiser¹⁵ and Parfitt and Smart.^{10,11} The similarity to previously published experimental IR spectra and the presence of four bands (one attributed to the ν_1 fundamental and three to the ν_3 fundamental) led to the assertion that sulfate adsorbed to Fe–(hydr)oxide surfaces predominantly formed a bidentate bridging complex.¹⁴

Recent investigations have been performed with in situ IR spectroscopy, namely the attenuated total reflectance Fourier transform infrared (ATR-FTIR) method.^{16,17} The ATR-FTIR method provides the capability of collecting real-time measurements and probing the speciation and coordination of molecules at hydrated mineral surfaces. Hug¹⁶ investigated sulfate adsorption to α -Fe₂O₃ using ATR-FTIR as a function of reactant concentration ($1 < x < 2000 \mu\text{M}$) and pH ($3 < x < 7$). The ATR-FTIR spectra showed an active ν_1 fundamental and a ν_3 fundamental split into two distinct bands. On the basis of the number of bands observed, a monodentate (C_{3v}) surface complex was assigned from the experimental results.¹⁶

Prior to the research of Hug,¹⁶ the majority of IR measurements of sulfate adsorbed to mineral surfaces used dried samples,^{10,11,14,15} and the prevalent structural assignment was a bidentate bridging complex on the basis of four observed IR-active bands. Hug¹⁶ proposed a hypothesis concerning the observation of a fourth band, namely that sample drying may lead to modifications of sulfate coordination or speciation. Measurements of dried sulfate-treated α -Fe₂O₃ at pH 3.6 showed an IR band at $\sim 1200 \text{ cm}^{-1}$, and the intensity of this band increased upon further drying with N₂(g).¹⁶ The band at $\sim 1200 \text{ cm}^{-1}$ also appeared with α -Fe₂O₃ in contact with aqueous sulfate solutions acidified below pH 2, leading to speculation that the speciation of sulfate was modified.

The ATR-FTIR results of Hug¹⁶ demonstrate the need to explore the effect of (de)hydration on sulfate speciation and coordination to Fe–(hydr)oxide surfaces. An understanding of the consequences of dehydration at the mineral–water interface on the coordination and speciation of surface-bound oxyanions is crucial with respect to predicting their bioavailability and transport in geochemical and soil systems. The objective of the present investigation was to utilize molecular orbital/density functional theory (MO/DFT) frequency calculations to unravel the relationship between Fe–(hydr)oxide surface (de)hydration and sulfate speciation and coordination. MO/DFT frequency calculations are useful for interpreting complicated IR spectra of oxyanions adsorbed to mineral

surfaces and are not susceptible to the shortcomings of qualitative group theory-based symmetry arguments and interpretations.^{18–20} The present investigation specifically addressed the following questions raised by Hug:¹⁶ (1) Does Fe–(hydr)oxide surface dehydration cause a conversion of adsorbed sulfate to bisulfate (i.e., speciation change) or (2) does surface dehydration cause a conversion from a monodentate to bidentate bridging adsorption complex (i.e., coordination change) or potentially a combination of both?

This investigation also addresses the potential importance of H-bonded sulfate adsorption. MO/DFT frequency calculations were performed in order to predict optimized geometries and IR spectra that correspond to potential adsorption complexes of sulfate and bisulfate at the Fe–(hydr)oxide–H₂O interface. The MO/DFT calculated frequencies were compared to available literature results and ATR-FTIR results of sulfate adsorbed at the α -Fe₂O₃–H₂O interface collected in our laboratory.

2. Materials and Methods

2.1. Experimental Methods. **2.1.1. Mineral Synthesis and Characterization.** Synthetic α -Fe₂O₃ was prepared following a method of Schwertmann and Cornell.²¹ Briefly, 500 mL of a 0.2 M Fe(CIO₄)₃ solution was heated to 98 °C for 7 days. The product was centrifuged and washed several times using ultrapure DI water, freeze-dried, and stored in the dark as a powder. Powder X-ray diffraction verified that the synthetic product was α -Fe₂O₃ and free of impurities. The Brunauer, Emmett, Teller measured surface area was $47.8 \text{ m}^2/\text{g} \pm 0.5 \text{ m}^2/\text{g}$ (sample degassed overnight at 100 °C) and the total pore volume was $0.074 \text{ cm}^3/\text{g}$.

2.1.2. ATR-FTIR Spectroscopy and Data Analysis. Infrared measurements were performed using a Thermo Electron NEXUS 670 FTIR spectrometer equipped with a PIKE Technologies horizontal attenuated total reflectance (HATR) flow-through accessory and a germanium (Ge) internal reflection element (IRE). The HATR flow-through accessory has a 100 μL solution cell volume, and both the IRE and the top plate are sealed using inert Teflon-coated gaskets. This setup produces an aqueous film that flows across the mineral surface with limited turbulence. A liquid nitrogen-cooled mercury cadmium telluride (MCT-A) detector was utilized to collect high-resolution spectra in the wavenumber region of interest ($1350\text{--}900 \text{ cm}^{-1}$). Spectra were collected using 128 co-added scans at 8 cm^{-1} resolution.

A thin Fe₂O₃ film was adhered to the Ge IRE by allowing 200 μL of a 40 g/L α -Fe₂O₃ slurry ($\sim 8 \text{ mg}$ solid before rinsing) to dry on the IRE in a 70:30 water/ethanol solution. After drying, the film was rinsed a minimum of three times with DI H₂O adjusted to pH 4.0 using HCl. A 1 mL aliquot of rinse solution was pipetted across the film and collected as waste. Rinsing removed any particles that were not in intimate contact with the IRE and would, therefore, not be probed by the infrared beam. After rinsing, the IRE was placed into the flow cell and sealed. The rinse solution was then pumped across the IRE surface, using a peristaltic pump set to a flow rate of $\sim 500 \mu\text{L}/\text{min}$, for $\sim 4 \text{ h}$ to allow for surface hydration and equilibration.

After hydration, a background spectrum was collected to produce a single-beam spectrum that samples the IRE, the atmosphere within the spectrometer, the α -Fe₂O₃ film, and the aqueous solution. After collecting the background spectrum, a second single-beam spectrum was collected and ratioed against the background, producing the baseline for the experiment. In principle, spectra collected beyond this point in time should only

(12) Nakamoto, K. *Infrared and Raman spectra of inorganic and coordination compounds*, 5th ed.; Wiley: New York, 1997.

(13) Carter, R. L. *Molecular symmetry and group theory*; J. Wiley: New York, 1998.

(14) Turner, L. J.; Kramer, J. R. *Soil Science* **1991**, *152*, 226.

(15) Harrison, J. B.; Berkheiser, V. E. *Clays Clay Miner.* **1982**, *30*, 97.

(16) Hug, S. J. *J. Colloid Interface Sci.* **1997**, *188*, 415.

(17) Peak, D.; Ford, R. G.; Sparks, D. L. *J. Colloid Interface Sci.* **1999**, *218*, 289.

(18) Myneni, S. C. B. X-ray and vibrational spectroscopy of sulfate in earth materials. In *Sulfate Minerals - Crystallography, Geochemistry and Environmental Significance*; Alpers, C. N., Jambor, J. L., Nordstrom, D. K., Eds.; Mineralogical Society of America: Washington, DC, 2000; Vol. 40, p 113.

(19) Rotzinger, F. P.; Kesselman-Truttmann, J. M.; Hug, S. J.; Shklover, V.; Gratzel, M. *J. Phys. Chem. B* **2004**, *108*, 5004.

(20) Kwon, K. D.; Kubicki, J. D. *Langmuir* **2004**, *20*, 9249.

(21) Schwertmann, U.; Cornell, R. M. *Iron oxides in the laboratory: preparation and characterization*; VCH: Weinheim; New York, 1991.

provide information about species introduced into the system that interact with the surface.

The input solution was switched to a 50 μM solution of Na_2SO_4 (pH 4.0) and was pumped into the reaction cell for ~ 1 h. A spectrum was collected every 5 min until the collected spectra superimposed. This condition represents the complete loading of $\alpha\text{-Fe}_2\text{O}_3$ surface sites with sulfate. After site saturation, the solution was switched back to the equilibration solution and allowed to flow for ~ 1 h to remove any sulfate remaining in solution from the reaction cell. No difference in the spectra before and after rinsing was seen. The spectrum shown in the results section is a spectrum collected after site saturation and rinsing.

An inverse second derivative spectrum (ISDS) was used to locate the peak positions in the sulfate adsorption experiment.²² The second-derivative test allows one to probe the peak maxima obtained from an absorption spectrum. Inversion of the second-derivative spectrum is simply done for easy comparison to absorbance data.²² Therefore, peak maxima in the ISDS correspond to peak maxima in the absorption spectrum. Because of the nature of the second-derivative test, no baseline correction was necessary for the collected spectrum.

To test the validity of ISDS-derived peak positions, nonlinear peak fitting was performed on the spectral data and a simple linear baseline correction was used for this alternate data set. Nonlinear peak fitting was performed using Origin 6.0. Multiple Gaussian or Lorentzian functions were used to fit the collected spectrum. Peak positions were set to the positions obtained from the ISDS, and a high-quality fit was obtained ($r^2 = 0.99$). A second fit procedure was performed to investigate the use of only three Gaussians, rather than the four established by the ISDS. This resulted in a lower quality of fit ($r^2 \approx 0.8$) and significantly larger full width at half-maximum (fwhm) values for the three peaks (data not shown). Peak center, amplitude, and fwhm parameters were allowed to float in order to establish the best fit of the data. Negative peaks were not allowed during the fitting procedure.

2.2. Theoretical Calculations. Cluster models constructed from two edge-sharing Fe(III) octahedra were used to simulate a generic Fe-(hydr)oxide surface, particularly the local coordination environment of adsorbed (bi)sulfate. Sulfate surface complexes representative of bidentate bridging, monodentate, and H-bonded, or bisulfate surface complexes representative of bidentate bridging and monodentate, respectively, were investigated. Cluster models are suitable approximations for surfaces of crystalline ionic solids because the geometry of the cutouts from the bulk generally maintains similar fully optimized cluster structures.²³

The overall charge of each sulfate-Fe(III) cluster was neutral (edge-sharing Fe(III) octahedra = + 2 and sulfate = -2) and each bisulfate-Fe(III) cluster + 1 (edge-sharing Fe(III) octahedra = + 2 and bisulfate = -1). These cluster model calculations simulate adsorption below the point of zero charge (i.e., mineral surface has a net positive charge density). To account for hydration and local asymmetrical H-bonding at the mineral-water interface, the supermolecule approach was taken whereby water molecules were explicitly positioned in proximity to the (bi)sulfate-Fe(III) cluster. Explicit consideration of water molecules in the cluster models is critical in order to capture the effect of short-range local and asymmetrical H-bonding of water to the O atoms of adsorbed sulfate²⁴ (O and H atoms of adsorbed bisulfate), which has been shown experimentally to affect the S-O vibrational frequencies.^{16,25}

To investigate the effect of (de)hydration on the calculated vibrational frequencies, the geometry of the bidentate bridging sulfate- and bisulfate-Fe(III) clusters were optimized with four and eight explicit water molecules. Explicit hydration of three to four waters was necessary to maintain cluster stability and prevent waters coordinated to Fe from migrating and forming H-bonds with (bi)sulfate. Therefore, (bi)sulfate surface complexes under totally dry conditions (no explicit waters coordinated to (bi)sulfate) could not be realistically modeled. Despite the simplicity of these cluster models, they have been shown to predict

optimized geometries and vibrational frequencies in agreement with experimental results.^{19,20,26-33}

All calculations were performed using the electronic structure program Gaussian 03.³⁴ The unrestricted hybrid density functional method was employed using Becke's 3-parameter nonlocal exchange functional^{35,36} with the gradient-corrected correlation functional of Lee-Yang-Parr³⁷ (UB3LYP). The standard 6-31+G(d) all-electron split valence basis set including polarization and diffuse functions on all non-hydrogen atoms was utilized. Additionally, the standard 6-311+G(d,p) all-electron triple split valence basis set was utilized for the bidentate bridging (bi)sulfate-Fe(III) clusters to test the effect of increased splitting of the valence orbitals and the addition of polarization functions to H atoms on the calculated vibrational frequencies.

Minima on the potential energy surfaces were located from a geometry optimization calculation on the entire system where no symmetry or geometrical constraints were allowed. Frequency calculations were subsequently performed on the geometry optimized structures corresponding to stationary points on the potential energy surface to verify that a minimum was successfully located (i.e., no imaginary frequencies) and to obtain predicted IR frequencies comparable to experimental IR spectra.

3. Results

3.1. ATR-FTIR Spectrum of Sulfate Adsorbed at the Hematite-Water Interface. Figure 1 shows the ATR-FTIR spectrum of the S-O stretching region (1350-900 cm^{-1}) measured for sulfate adsorbed to a hydrated $\alpha\text{-Fe}_2\text{O}_3$ surface at maximum surface loading. It should be noted that, compared to Figure 1, spectra collected before maximum surface loading only differed in absorbance intensity (i.e., the number of measured bands and their positions did not change as a function of surface loading). The corresponding band positions, determined from the maxima of the inverse second-derivative spectrum (red spectrum in Figure 1), are listed in Table 1. After maximum surface loading had been achieved, water adjusted to pH 4 was pumped across the $\alpha\text{-Fe}_2\text{O}_3$ surface to remove any sulfate remaining in solution from the reaction cell.

(26) Kubicki, J. D.; Apitz, S. E. *Am. Mineral.* **1998**, *83*, 1054.

(27) Kubicki, J. D.; Blake, G. A.; Apitz, S. E. *Geochim. Cosmochim. Acta* **1997**, *61*, 1031.

(28) Kubicki, J. D.; Itoh, M. J.; Schroeter, L. M.; Apitz, S. E. *Environ. Sci. Technol.* **1997**, *31*, 1151.

(29) Kubicki, J. D.; Schroeter, L. M.; Itoh, M. J.; Nguyen, B. N.; Apitz, S. E. *Geochim. Cosmochim. Acta* **1999**, *63*, 2709.

(30) Sainz-Diaz, C. I.; Timon, V.; Botella, V.; Hernandez-Laguna, A. *Am. Mineral.* **2000**, *85*, 1038.

(31) Sherman, D. M.; Randall, S. R. *Geochim. Cosmochim. Acta* **2003**, *67*, 4223.

(32) Yoon, T. H.; Johnson, S. B.; Musgrave, C. B.; Brown, G. E. *Geochim. Cosmochim. Acta* **2004**, *68*, 4505.

(33) Zhang, N. L.; Blowers, P.; Farrell, J. *Environ. Sci. Technol.* **2005**, *39*, 4816.

(34) Frisch, M. J.; Trucks, G. W.; Schlegel, H. B.; Scuseria, G. E.; Robb, M. A.; Cheeseman, J. R.; Montgomery, J. A., Jr.; Vreven, T.; Kudin, K. N.; Burant, J. C.; Millam, J. M.; Iyengar, S. S.; Tomasi, J.; Barone, V.; Mennucci, B.; Cossi, M.; Scalmani, G.; Rega, N.; Petersson, G. A.; Nakatsuji, H.; Hada, M.; Ehara, M.; Toyota, K.; Fukuda, R.; Hasegawa, J.; Ishida, M.; Nakajima, T.; Honda, Y.; Kitao, O.; Nakai, H.; Klene, M.; Li, X.; Knox, J. E.; Hratchian, H. P.; Cross, J. B.; Bakken, V.; Adamo, C.; Jaramillo, J.; Gomperts, R.; Stratmann, R. E.; Yazyev, O.; Austin, A. J.; Cammi, R.; Pomelli, C.; Ochterski, J. W.; Ayala, P. Y.; Morokuma, K.; Voth, G. A.; Salvador, P.; Dannenberg, J. J.; Zakrzewski, V. G.; Dapprich, S.; Daniels, A. D.; Strain, M. C.; Farkas, O.; Malick, D. K.; Rabuck, A. D.; Raghavachari, K.; Foresman, J. B.; Ortiz, J. V.; Cui, Q.; Baboul, A. G.; Clifford, S.; Cioslowski, J.; Stefanov, B. B.; Liu, G.; Liashenko, A.; Piskorz, P.; Komaromi, I.; Martin, R. L.; Fox, D. J.; Keith, T.; Al-Laham, M. A.; Peng, C. Y.; Nanayakkara, A.; Challacombe, M.; Gill, P. M. W.; Johnson, B.; Chen, W.; Wong, M. W.; Gonzalez, C.; Pople, J. A. *Gaussian 03*, revisions B.02 and C.01; Gaussian, Inc.: Wallingford, CT, 2004.

(35) Stephens, P. J.; Devlin, F. J.; Chabalowski, C. F.; Frisch, M. J. *J. Phys. Chem.* **1994**, *98*, 11623.

(36) Becke, A. D. *J. Chem. Phys.* **1993**, *98*, 5648.

(37) Lee, C. T.; Yang, W. T.; Parr, R. G. *Phys. Rev. B* **1988**, *37*, 785.

(22) Persson, P.; Axe, K. *Geochim. Cosmochim. Acta* **2005**, *69*, 541.

(23) Jug, K.; Bredow, T. *J. Comput. Chem.* **2004**, *25*, 1551.

(24) Gao, B.; Liu, Z. F. *J. Chem. Phys.* **2004**, *121*, 8299.

(25) Myneni, S. C. B.; Traina, S. J.; Waychunas, G. A.; Logan, T. J. *Geochim. Cosmochim. Acta* **1998**, *62*, 3285.

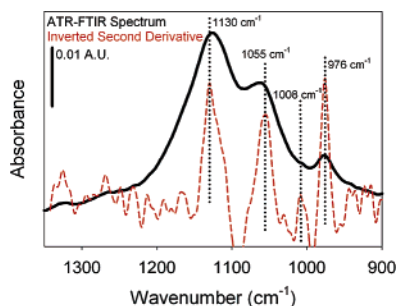


Figure 1. ATR-FTIR spectrum corresponding to the S–O stretching region (1350–900 cm^{-1}) of sulfate adsorbed to a hydrated hematite surface at pH 4.0. Solid black line corresponds to the ATR-FTIR spectrum. Red dotted line corresponds to the inverse second-derivative spectrum.

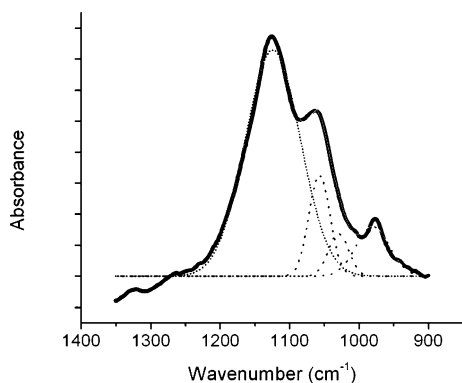


Figure 2. ATR-FTIR baseline-corrected spectrum corresponding to the S–O stretching region (1350–900 cm^{-1}) of sulfate adsorbed to a hydrated hematite surface at pH 4.0. Solid black line corresponds to the baseline-corrected ATR-FTIR spectrum. Thin dotted lines are Gaussian functions used to fit the overlapping normal modes in the spectrum, and the solid gray line superimposed on the experimental spectrum is the composite fit of all Gaussian functions.

Table 1. Experimental ATR-FTIR Frequencies (cm^{-1}) of Sulfate Adsorbed at the Hematite–Water Interface (pH 4.0), as Determined by the Inverse Second-Derivative Spectrum and Nonlinear Peak Fitting Using Gaussian Functions (Lorentzian Functions in Parentheses)

nonlinear peak fit ($r^2=0.99$)	inverse second derivative
1124 (1128)	1130
1057 (1060)	1055
1029 (1040)	1008
980 (974)	976

Relative to the band at 1008 cm^{-1} , three other bands corresponding to S–O normal modes measured at approximately 1130, 1055, and 976 cm^{-1} have comparatively larger intensities (Table 1, Figure 1). To test if the band at 1008 cm^{-1} was real (or noise), the ATR-FTIR spectrum in Figure 1 was subjected to nonlinear curve fitting (the peak positions determined by the ISDS were used as input parameters for the fit). Figure 2 shows the nonlinear curve-fitted ATR-FTIR spectrum, and the corresponding frequencies of Gaussian peak maxima are listed in Table 1 (values in parentheses correspond to Lorentzian peak maxima from a separate nonlinear curve fit). The nonlinear curve-fitted frequencies (Gaussian peak maxima) are close to the frequencies determined by the ISDS with a mean difference of 8 cm^{-1} . This small difference is likely due to the inexact determination of peak maxima using both ISDS and nonlinear peak fitting. The ATR-FTIR spectrum in Figure 1 was also subjected to a fit using only three Gaussian peaks, which resulted in substantial

Table 2. Theoretical Vibrational Frequencies (cm^{-1}) of Potential Energy Minimized (bi)sulfate Surface Complexes on Fe(III)–(Hydro)oxide Clusters (UB3LYP/6-31G+(d))^a

sulfate			bisulfate	
BB	M	H-bonded	BB	M
			1236 (347)	1222 (307)
		1157 (336)	1152 (317)	1174 (282)
1143 (468)	1139 (338)	1128 (387)	1119 (243)	1105 (238)
1070 (423)	1043 (426)	1060 (376)		
1032 (183)	1006 (245)		1012 (266)	1011 (294)
988 (350)		976 (451)		
937 (45)	942 (171)	900 (248)		

^a Intensities are given in parentheses. BB, bidentate bridging; M, monodentate.

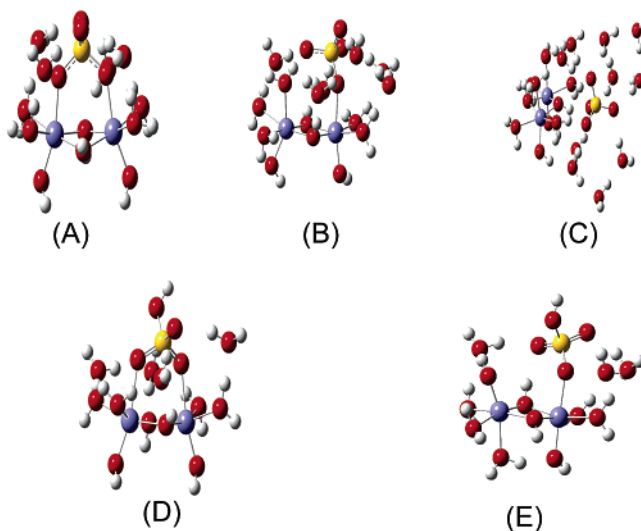


Figure 3. Potential energy minimized (bi)sulfate adsorption complexes on Fe(III) clusters: (A) sulfate bidentate bridging; (B) sulfate monodentate; (C) sulfate H-bonded; (D) bisulfate bidentate bridging; and (E) bisulfate monodentate. H_2O molecules explicitly considered in all calculations are H-bonded to the (bi)sulfate cluster models (H-bonded optimized with 10 H_2O molecules). Calculations were performed at the UB3LYP/6-31+G(d) level of theory. Red, oxygen; white, hydrogen; yellow, sulfur; blue, iron.

reduction to the fit quality ($r^2 = 0.99 \rightarrow \sim 0.8$; data not shown). Therefore, four bands corresponding to S–O normal modes for sulfate adsorbed at the $\alpha\text{-Fe}_2\text{O}_3$ –water interface have been identified. This finding differs with the results of Hug¹⁶ who identified three bands and will be examined in the Discussion.

3.2. MO/DFT Frequency Calculations. The calculated vibrational frequencies of the (bi)sulfate–Fe(III) clusters are listed in Table 2, and their corresponding molecular structures are depicted in Figure 3. In each case, all frequencies are real and the stationary points on the potential energy surfaces correspond to local energy minima. Each (bi)sulfate configuration is distinguishable due to the different number and energy of predicted frequencies, facilitating their comparison to experimental data and possible assignment of surface complexes. The calculated vibrational frequencies contained in Table 2 for the monodentate structures have been improved from values that we have concurrently published.³⁸

The accuracy of the total electronic wave function and its effect on the predicted vibrational frequencies was

(38) Usher, C. R.; Paul, K. W.; Narayansamy, J.; Kubicki, J. D.; Sparks, D. L.; Schoonen, M. A. A.; Strongin, D. R. *Environ. Sci. Technol.* 2005, web release.

Table 3. Theoretical Vibrational Frequencies (cm^{-1}) of Potential Energy Minimized Bidentate Bridging Fe(III) Sulfate and Bisulfate Clusters Calculated at the UB3LYP/6-311+G(d,p) Level of Theory

bidentate bridging sulfate	bidentate bridging bisulfate
	1227 (394)
1137 (484)	1143 (400)
	1111 (168)
1067 (560)	
1013 (416)	1014 (227)
957 (269) ^b	
945 (52)	

^a Intensities are given in parentheses. ^b Reduction in atomic displacement relative to 988 cm^{-1} spectral line predicted at UB3LYP/6-31+G(d) level of theory (Table 2).

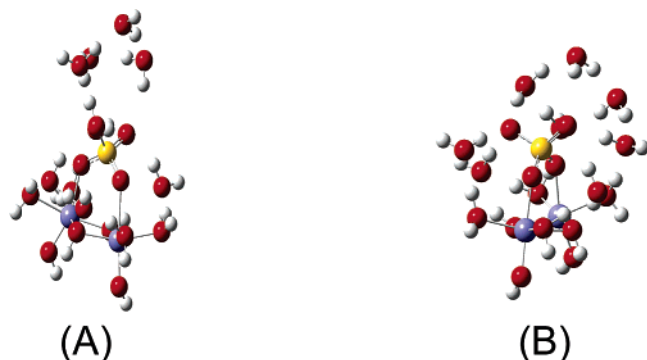


Figure 4. Potential energy minimized (bi)sulfate adsorption complexes on Fe (III) clusters using eight explicit H_2O molecules: (A) bisulfate bidentate bridging; (B) sulfate bidentate bridging. Calculations were performed at the UB3LYP/6-31+G(d) level of theory. Red, oxygen; white, hydrogen; yellow, sulfur; blue, iron.

tested by using the 6-311+G(d,p) basis set to re-optimize the bidentate bridging Fe(III) sulfate and bisulfate clusters (Figure 3, A and D, respectively) previously optimized at the UB3LYP/6-31+G(d) level of theory (i.e., test the effect of increased valence orbital splitting and the addition of polarization functions on the H atoms). Table 3 lists the calculated vibrational frequencies of the bidentate bridging Fe(III) sulfate and bisulfate clusters optimized at the UB3LYP/6-311+G(d,p) level of theory. A comparison of the vibrational frequencies calculated using the 6-31+G(d) versus 6-311+G(d,p) basis sets (Tables 2 and 3, respectively) revealed the larger basis set results in only modest shifts of the frequencies (15 and 7 cm^{-1} for the bidentate bridging sulfate and bisulfate clusters, respectively). This result illustrates a reduction in computational cost may be achieved without sacrificing the accuracy of the predicted IR vibrational frequencies with respect to the size of an all-electron basis set. Furthermore, experimental IR S–O stretching frequencies associated with adsorbed (bi)sulfate at the Fe–(hydr)oxide- H_2O interface are estimations typically derived from nonlinear curve fitting or simply by visual inspection. Therefore, in the remainder of this manuscript, the theoretical results in Table 2 will be used to compare to experimental IR frequencies presented in the Discussion section.

To investigate the effect of reverse dehydration on the calculated vibrational frequencies, the optimized geometries of the bidentate bridging sulfate and bisulfate clusters (Figure 2, A and D, respectively; four explicit waters) were re-optimized with eight explicit water molecules. Figure 4 depicts these optimized geometries, and their vibrational frequencies are listed in Table 4. A comparison between the MO/DFT calculated vibrational

Table 4. Theoretical Vibrational Frequencies (cm^{-1}) of Potential Energy Minimized Bidentate Bridging Fe(III) Sulfate and Bisulfate Clusters Calculated at the UB3LYP/6-31+G(d) Level of Theory Including Eight Explicit Water Molecules

bidentate bridging sulfate	bidentate bridging bisulfate
	1354 (153) ^a
	1164 (428)
1120 (421)	1132 (240) ^a
1057 (293)	1112 (292)
1040 (513)	1011 (348)
988 (306)	947, 988 (20, 60) ^a
931 (28)	884, 886 (223, 203) ^a
	856 (203)

^a Predicted S–O(H) stretching frequencies coupled to extra water molecules not previously calculated in the bidentate bridging bisulfate structure (four waters).

Table 5. Experimental ATR-FTIR Frequencies (cm^{-1}) of Sulfate Complexes Adsorbed to Hematite^a and Goethite^b under a Variety of Experimental Conditions

100 μM , pH 3 ^a	20 μM , pH 4 ^a	dry ^a	20 μM , pH 3.5–5.5 ^b
		1199	
			1170
1130	1128	1131	1133
			1108 ^c
1052	1057	1057	1055
			992
975	975	975	975 ^c

^a Hug.¹⁶ ^b Peak et al.¹⁷ ^c Attributed to an outer-sphere complex by authors.

frequencies for the bidentate bridging sulfate structure (Figure 3A and Figure 4B, Tables 2 and 4, respectively) using four and eight explicit waters reveals minor frequency shifts (average of 10 cm^{-1}). This is not unexpected because adding four additional waters simply increases the number of hydrogen bonds to the sulfate oxygen atoms. On the other hand, significant changes result when the bidentate bridging bisulfate structure with only four H_2O molecules is re-optimized with four extra H_2O molecules (Figure 4A). With only four waters, the hydrogen in bisulfate (Figure 3D) is not participating in hydrogen bonding (this scenario represents a ‘dried’ Fe–(hydr)oxide surface where sulfate has undergone a speciation change to form bisulfate and will be discussed in the next section). However, with eight waters, several new frequencies are predicted that correspond to bisulfate normal modes coupled to the extra waters (Table 4). Most importantly, when eight waters are considered, substantial weakening of the O–H bond in bisulfate occurs (increase in bond length from 0.977 to 1.034 Å).

4. Discussion

Sulfate adsorption to $\alpha\text{-Fe}_2\text{O}_3$ ¹⁶ and $\alpha\text{-FeOOH}$ ¹⁷ has been investigated using ATR-FTIR under in situ (aqueous) conditions, and experimental frequencies for these particular studies are reported in Table 5. At pH 3 (100 μM SO_4^{2-}) and 4 (20 μM SO_4^{2-}), Hug¹⁶ reported a monodentate sulfate complex formed at the $\alpha\text{-Fe}_2\text{O}_3$ surface under hydrated conditions. The surface complex assignment was based upon the observation of three IR-active bands, suggestive of a C_{3v} monodentate complex from a group theoretical analysis (i.e., IR-active ν_1 fundamental and ν_3 fundamental split into two bands). In Table 2, the calculated frequencies for monodentate sulfate at 1043 and 1006 cm^{-1} arise from an identical normal mode and the intensity weighted average equals 1029 cm^{-1} . A comparison of the experimental frequencies under hy-

drated conditions at pH 3 and 4 (Table 5) and the MO/DFT calculated frequencies (Table 2) for monodentate sulfate reveals a good agreement, with the exception that the symmetric stretching mode at 942 cm^{-1} is underestimated.

In our ATR-FTIR experiments of sulfate adsorbed at the $\alpha\text{-Fe}_2\text{O}_3$ -water interface, four bands were identified by means of both the inverse second derivative and nonlinear peak-fitted spectra (Table 1, Figures 1 and 2). In Table 2, the calculated frequencies for bidentate bridging sulfate at 1032 and 988 cm^{-1} arise from an identical normal mode and the intensity-weighted average equals 1003 cm^{-1} . Comparison of our experimental frequencies under hydrated conditions at pH 4 (Table 1) and the MO/DFT calculated frequencies (Table 2) for bidentate bridging sulfate reveals a good agreement, again with the exception that the symmetric stretching mode at 937 cm^{-1} is underestimated. Another reasonable surface complex that may be present under our and Hug's experimental conditions (Tables 1 and 5, respectively) is H-bonded sulfate. In Table 2, the calculated frequencies at 1157 and 1128 cm^{-1} arise from an identical normal mode and the intensity-weighted average equals 1141 cm^{-1} . The two lowest-energy predicted frequencies at 976 and 900 cm^{-1} (Table 2) both dramatically underestimate the experimental frequencies (Table 1). Thus, a simple linear regression analysis of the theoretical frequencies (Table 2) versus our experimental frequencies (Table 1) reveals that bidentate bridging sulfate is a better assignment than H-bonded sulfate.

An important difference between our experimental data and those of Hug is the number of identified bands which results in different surface complex assignments. If an unidentified band at $1000 \leq x \leq 1040\text{ cm}^{-1}$ were present in Hug's spectra (as it is in ours), then a bidentate bridging sulfate complex is currently the most reasonable surface complex assignment. Unfortunately, distinguishing between the monodentate and bidentate bridging coordination geometries may be exceedingly difficult using the ATR-FTIR technique, where the resolution of the FTIR data becomes critical. The discrepancy in the number of measured bands between these two investigations may also arise from differences in surface loading of sulfate on the hematite particle surfaces.

Upon drying, the sulfate surface complex changes, as indicated by the experimental frequencies reported by Hug¹⁶ in Table 5. Hug¹⁶ hypothesized the appearance of a fourth band at or above 1200 cm^{-1} may be the result of a change in speciation (sulfate to bisulfate conversion) or a change in coordination (monodentate-to-bidentate bridging structural conversion). On the basis of the preceding arguments, a change in coordination from a monodentate to bidentate bridging sulfate structure is ruled out because the assignment based upon the MO/DFT results is likely one of these two complexes under hydrated conditions. A comparison of the MO/DFT results in Table 2 and the ATR-FTIR results for the drying experiment in Table 5 reveal a speciation change is credible (i.e., bidentate bridging or monodentate sulfate conversion to bidentate bridging and/or monodentate bisulfate). The three experimental frequencies less than 1200 cm^{-1} (Table 5) roughly maintain their position with respect to the pH 3 and 4 spectra of the hydrated bidentate bridging sulfate complex, suggesting that a fraction of the surface complex remains post-drying. It is likely that a mixture of sulfate and bisulfate exists at the $\alpha\text{-Fe}_2\text{O}_3$ surface under dry conditions with five observed bands, one above 1200 cm^{-1} arising from sulfate protonation and conversion to bisulfate.

The bisulfate O-H bond length substantially increases from 0.977 to 1.034 \AA when the bidentate bridging bisulfate geometry optimized with four explicit waters (Figure 3D) is re-optimized with eight explicit waters (Figure 4A). Essentially, this optimized structure represents a reverse 'snapshot' along the reaction path whereby sulfate changes speciation to bisulfate (i.e., sulfate is protonated) upon drying. The weakening of the bisulfate O-H bond (i.e., increase in bond distance) as displayed by the MO/DFT results suggests that the change in speciation upon drying (or rewetting) is reversible. In other words, when sulfate, adsorbed as a bidentate bridging or monodentate structure under hydrated conditions, changes speciation and converts to bisulfate as a function of drying, the speciation change is reversible (i.e., upon rewetting, bisulfate is converted back to sulfate). Unfortunately, the MO/DFT geometry optimizations are calculated for static structures and the full dynamical effect of this process is impossible to explore using static MO/DFT calculations (this explains why the predicted frequencies for the bisulfate structure in Table 3 do not correspond to an experimental equilibrium adsorption complex because this structure is not a reaction product). However, a theoretical investigation of this dynamical process may be amenable to *ab initio* molecular dynamics and is the subject of future research.

Table 5 also contains ATR-FTIR experimental frequencies corresponding to sulfate adsorption on $\alpha\text{-FeOOH}$ between pH 3.5 and 5.5.¹⁷ Peak et al.¹⁷ assigned the sulfate surface complex as a monodentate bisulfate or monodentate sulfate (plus H-bonding to an adjacent surface site) structure, in addition to an outer-sphere component (1108 and 975 cm^{-1} in Table 5). Upon comparison of the MO/DFT calculated frequencies (Table 2) for the monodentate bisulfate and the experimental frequencies (Table 5, last column), it is evident a discrepancy exists between the assigned structure and its corresponding calculated frequencies. The monodentate bisulfate structure is predicted to have an active asymmetric IR stretching mode greater than 1200 cm^{-1} , a diagnostic feature absent in the experimental spectra.

Peak et al.¹⁷ identified four bands in their experimental spectra that were assigned as inner-sphere (Table 5), reasoning that monodentate sulfate may form an H-bond to an adjacent surface site (i.e. C_{2v} structure). When sulfate forms a monodentate surface complex under hydrated conditions, it is difficult to imagine that it would not simultaneously undergo H-bonding with an adjacent surface OH or H_2O functional group given the proximity of the complex to an adjacent surface site. The geometry-optimized monodentate sulfate complex (Table 2, Figure 3) formed an H-bond to the adjacent surface H_2O functional group. Comparing the calculated frequencies of monodentate sulfate (Table 2) and the experimental frequencies in Table 5 reveals that this assignment may be incorrect because monodentate sulfate is predicted to have only three IR-active normal modes, regardless of whether it forms an H-bond to an adjacent surface site. Both bidentate bridging and H-bonded sulfate are predicted to have four IR-active normal modes (Table 2) and may better explain the observed experimental spectra. Unfortunately, in the current investigation, it was not possible to explore the possibility of outer-sphere complexes where one or more monolayers of water (full hydration shells) separate sulfate from the cluster due to computational cost considerations.

Before the use of ATR-FTIR became routine in aqueous mineral surface geochemical applications, several investigations were conducted on sulfate sorption to Fe-(hydr)-oxides using transmission and diffuse reflectance IR

Table 6. Experimental IR (ex situ) Frequencies (cm^{-1}) of Sulfate Complexes Adsorbed to Hematite^a and Goethite^b

hematite ^a	goethite ^b
1255	1250
1130	1130
1030	1050
950	980

^a Turner and Kramer.¹⁴ ^b Persson and Lovgren.³⁹**Table 7. Experimental IR (ex situ) Frequencies (cm^{-1}) of Sulfate Complexes Adsorbed to Hematite, Goethite, Akaganeite, and Lepidocrocite^a**

hematite	goethite	akaganeite	lepidocrocite
1200 (1245)	1254 (1282)	1200 (1215)	1250 (1275)
1128 (1131)	1141 (1150)	1120 (1123)	1133 (1140)
1040 (1030)	1040 (955)	1060 (1035)	^b
970 (950)	965 (909)	970 (950)	965 (955)

^a Values in parentheses correspond to evacuated samples and the other values correspond to air-dry samples. Parfitt and Smart.¹¹ ^b Reported as obscured.

spectroscopy.^{11,14,15,39} Unfortunately, the experiments involved different variables and conditions under which spectra were collected, essentially making direct comparisons exceedingly difficult or altogether impossible. For the purposes of this discussion, the MO/DFT calculated frequencies will not be compared to the work of Harrison and Berkheiser¹⁵ because their experiments were performed such that sulfate was occluded in the crystalline structure of their hydrous iron oxides (i.e., not strictly surface complexes).

Table 6 lists the results of experiments conducted by Turner and Kramer¹⁴ and Persson and Lovgren.³⁹ Turner and Kramer¹⁴ interpreted their spectra as sulfate forming a bidentate bridging complex on $\alpha\text{-Fe}_2\text{O}_3$. Clearly, a bidentate bridging sulfate complex is not the only complex in their system because the band at 1255 cm^{-1} (Table 6, first column) does not correspond to this assigned structure in consideration of the MO/DFT calculated frequencies (Table 2). Their spectra are similar to those of Hug¹⁶ with a single high-energy band greater than 1200 cm^{-1} and approximately three lower-energy bands: roughly 1130 and 1130, 1030 and 1050, and 950 and 975 cm^{-1} for Turner and Kramer¹⁴ and Hug,¹⁶ respectively. As previously mentioned these similarities show that bidentate bridging or monodentate sulfate, upon drying, likely changes speciation and forms bidentate bridging and/or monodentate bisulfate in a mixture of unknown proportion (i.e., not 100% conversion).

Persson and Lovgren³⁹ interpreted their spectra as an outer-sphere sulfate complex forming at the surface of $\alpha\text{-FeOOH}$. Their measured frequencies are similar to those of Turner and Kramer¹⁴ (Table 6), qualitatively suggesting that the same surface complex is present on both dried $\alpha\text{-Fe}_2\text{O}_3$ and $\alpha\text{-FeOOH}$ samples. Persson and Lovgren³⁹ also suggested the presence of protonated sulfate at the goethite surface below pH 5, which is in line with the MO/DFT results for the bidentate bridging and/or monodentate bisulfate structure.

Parfitt and Smart¹¹ used transmission IR spectroscopy to measure the interaction of sulfate with several air-dried and evacuated Fe-(hydr)oxide mineral surfaces, and these experimental results are listed in Table 7. The proposed surface complex for sulfate on all of the Fe-(hydr)oxide surfaces was a bidentate bridging structure. Upon evacuation, the experimental frequencies undergo

shifts of varying degree depending on the specific structure of the mineral surface, but the nature of adsorbed (bi)sulfate does not change with respect to speciation or coordination.¹¹ Similar to the proposed structural assignment of Turner and Kramer,¹⁴ Parfitt and Smart¹¹ assigned their spectra solely to the presence of a bidentate bridging sulfate complex. With respect to the MO/DFT calculated frequencies (Table 2), a mixture of bidentate bridging and monodentate sulfate and bisulfate likely exists under their experimental conditions, similar to the results of Turner and Kramer,¹⁴ Hug,¹⁶ and Persson and Lovgren.³⁹

5. Conclusions

MO/DFT frequency calculations were utilized to investigate the effect of dehydration on the equilibrium surface complexes of (bi)sulfate at the Fe-(hydr)oxide- H_2O interface. Though this investigation has not unequivocally determined the exact nature of (bi)sulfate at the (de)hydrated Fe-(hydr)oxide surface, the following general sequence is proposed. (1) At the Fe-(hydr)oxide- H_2O interface, sulfate adsorbs as a bidentate bridging or monodentate surface complex under most experimental conditions. (2) Upon dehydration, proton accumulation causes a speciation change: bidentate bridging or monodentate sulfate converts to bidentate bridging and/or monodentate bisulfate. An undetermined distribution of both sulfate and bisulfate exists. In other words, the speciation change does not yield 100% conversion. (3) The speciation change is reversible as a function of rehydration.

The MO/DFT results were compared to several experimental studies which had assigned the (bi)sulfate surface geometry using a group theoretical analysis. Within the framework of a group theoretical analysis, the symmetry of a molecule, or complex ion, is explicitly considered, without consideration of the symmetry that results from associations and interactions with neighboring molecules.¹³ Sulfate adsorbed to a mineral surface is unlikely to preserve a well-defined high-symmetry point group (i.e., descent in symmetry of the T_d point group through its hierarchy of subgroups— C_{3v} , C_{2v} , etc.) with respect to its metal complex counterparts in solution. At a mineral surface, structural distortion is expected to occur due to electrical double-layer influences and local asymmetrical hydrogen-bonding from surface hydration, ultimately leading to nonideal behavior. Despite its limitations in helping to interpret spectra of adsorbed species at the mineral-water interface, group theory is an invaluable tool as a first approximation and provides an excellent qualitative view of the relationships between symmetry and surface complexation. However, it should be used cautiously as it treats the mineral-water interface in an ideal manner, neglecting such effects as strong H-bonding and electrical double-layer influences which may ultimately cause symmetry arguments to fail.

Though this investigation has revealed new insight into the nature of (bi)sulfate complexes at the Fe-(hydr)oxide-water interface, the processes explored herein are only indirect consequences of a more fundamental issue. The question of why particular mineral surfaces accumulate acidity upon dehydration needs to be addressed in order to predict the effects this process has on adsorption, mineral dissolution, microbial interactions, etc. Thermodynamic calculations aimed at exploring how the change in surface dielectric constant due to drying impacts oxyanion surface complexation (both coordination and speciation) should be performed. Also, future research coupling MO/DFT and IR spectroscopy to study the effect

(39) Persson, P.; Lovgren, L. *Geochim. Cosmochim. Acta* **1996**, *60*, 2789.

of mineral surface dehydration on the bioavailability and transport of other important oxyanions will be helpful with respect to improving surface complexation models.

Acknowledgment. The senior author appreciates the support of a USDA National Needs Graduate Fellowship. Computation was supported in part by the Materials Simulation Center, a Penn-State MRSEC, and MRI facility, as well as the Delaware Biotechnology Institute,

Bioinformatics Center (Douglas O'Neal, Manager). We appreciate the helpful editorial suggestions made by Ryan Tappero. The authors are indebted to the Senior Editor Ralph G. Nuzzo and one anonymous reviewer whose comments and support greatly facilitated the improvement of this manuscript.

LA050648V